Limnol. Oceanogr., 48(1), 2003, 18–30

Effects of ultraviolet-B radiation and vertical mixing on nitrogen uptake by a natural planktonic community shifting from nitrate to silicic acid deficiency

Eric Fouilland,[1] *Michel Gosselin, and Behzad Mostajir*[2]
Institut des sciences de la mer (ISMER), Université du Québec à Rimouski, 310 allée des Ursulines, Rimouski, Québec G5L 3A1, Canada

Maurice Levasseur
Institut Maurice-Lamontagne, Pêches et Océans Canada, C.P. 1000, Mont-Joli, Québec G5H 3Z4, Canada

Jean-Pierre Chanut, Serge Demers, and Stephen de Mora[3]
Institut des sciences de la mer (ISMER), Université du Québec à Rimouski, 310 allée des Ursulines, Rimouski, Québec G5L 3A1, Canada

Abstract

We investigated the combined effects of mixing regimes and ultraviolet-B radiation (UVBR: 280–320 nm) on the uptake of nitrate, ammonium, and urea by an estuarine phytoplankton community during a 10-d mesocosm experiment in July 1997. The experiment was conducted in eight mesocosms (1,500 liters each) subjected to varying conditions of UVBR and mixing: (1) natural UVBR and fast mixing, (2) enhanced UVBR and fast mixing, (3) natural UVBR and slow mixing, and (4) enhanced UVBR and slow mixing. The study was carried out during a typical midsummer period of low nutrient concentrations. Throughout the experiment, the phytoplankton community was dominated by a mixed community composed mainly of centric diatoms, cyanobacteria, and prymnesiophytes, with larger algal cells (>5 μm) representing >70% of the total chlorophyll *a* biomass. The phytoplankton nutrient status changed over the experiment. Algal cells were nitrate-deficient until the occurrence of a nitrification event on day 7, and then became silicic acid–deficient. Mesocosms with different mixing rates showed significant differences in ambient nutrient concentrations, nitrogen uptake rates, and phytoplankton species composition. In general, no significant difference was detected between the N transport rates from samples incubated close to the surface and close to the bottom of the mesocosms, and no difference was detected between the UVBR treatments on all the other studied biological and chemical variables measured during the experiment. It is only under the slow mixing regime that the enhanced UVBR treatments significantly depress both the transport and the chlorophyll *a*–specific transport rates of dissolved organic nitrogen (urea). The UVBR effects observed only in the slow mixing regime could be a consequence of an inherent difference in the uptake capacity of the different communities under the two mixing regimes. Both nutrient conditions and mixing regime influenced the natural phytoplankton physiology and composition toward a community more sensitive to UVBR enhancement under a slower mixing regime.

The negative effects of ultraviolet radiation (UVR) on aquatic organisms have attracted attention recently as ultraviolet-B radiation (UVBR: 280–320 nm) at ground level increases in response to continuing stratospheric ozone depletion (Kerr and McElroy 1993). Solar UVBR has been shown to significantly impair phytoplankton photosynthesis in several ecosystems (e.g., Smith et al. 1992; Vincent and Roy 1993; Furgal and Smith 1997; Mousseau et al. 2000). UVBR is also known to disrupt membrane integrity and cell replication (*see* references in Furgal et al. 1998), to inhibit the uptake of inorganic and organic dissolved nitrogen (Behrenfeld et al. 1995; Fauchot et al. 2000) and to modify the activity of associated enzymes and the synthesis of specific amino acids (Döhler 1985).

Phytoplankton sensitivity to UVBR might be influenced

[1] To whom correspondence should be addressed. Present address: The Scottish Association for Marine Science (SAMS), Dunstaffnage Marine Laboratory, Dunbeg, Oban, Argyll, PA37 1QA Scotland (erfo@dml.ac.uk).

[2] Present address: Réseaux Trophiques Pélagiques (GRD 2476) and Écologie Microbienne des Milieux Aquatiques, Écosystèmes Lagunaires, UMR 5119 CNRS-Université Montpellier II, Case 093, Place E. Bataillon, 34095 Montpellier Cedex 5, France.

[3] Present address: IAEA—Marine Environment Laboratory, 4, Quai Antoine 1er—BP 800, MC 98012, Principality of Monaco.

Acknowledgments

We thank D. Bourget, S. Doiron, M.-È. Garneau, L. Zudaire, L. Pageau, J. Côté, and C. Belzile for field and laboratory assistance; H. Browman for the use of his spectroradiometer; N. Lafontaine and A. Weise for nutrient analyses; W. G. Harrison for use of his mass spectrometer; L. Harris for performing the stable isotopes analyses; S. Lessard for phytoplankton identification; and L. Mousseau, S. Roy, and two anonymous reviewers for their judicious comments on the manuscript.

This project was supported by grants from NSERC of Canada, Fonds FCAR of Québec, and FODAR (Fonds pour le développement et l'avancement de la recherche, Université du Québec) to M.G., M.L., S.D., and S. dM. and by financial support to M.L. from the Maurice Lamontagne Institute (Department of Fisheries and Oceans, Canada). E.F. received a postdoctoral fellowship from Ministère de l'Éducation du Québec.

This is a contribution to the research programs of the Institut des sciences de la mer de Rimouski and of the Maurice Lamontagne Institute.

by environmental and physiological factors, such as the nutrient supply and the nutrient status of cells. Turnover of proteins essential for phytoplankton to recover from UVBR-induced damage is possibly inhibited when nitrogen or other inorganic nutrients are limiting (Cullen and Lesser 1991; Behrenfeld et al. 1994; Lesser et al. 1994). Planktonic organisms can perform short-term vertical displacements in the water column through vertical mixing or migration. These displacements alter their exposition to UVBR and change their response to this stress (Helbling et al. 1994; Jeffrey et al. 1996; Neale et al. 1998). Helbling et al. (1994) demonstrated experimentally that different vertical mixing regimes could modulate photosynthesis inhibition in Antarctic phytoplankton. When the timescale for biological response to the different light intensities is shorter than that for vertical mixing, phytoplankton exhibit a vertical gradient of photoacclimation (Lewis et al. 1984; Cullen and Lewis 1988). These observed effects of mixing on photosynthesis inhibition are consistent with the hypothesis that the response of phytoplankton to UVR depends on the history of UVR exposure during the day (dose) rather than on instantaneous UV irradiance (dose rate) (Cullen and Lesser 1991). On the basis of a biological model of UV-influenced photosynthesis in the presence of vertical mixing, Neale et al. (1998) concluded that photosynthesis inhibition by near-surface UVR can be enhanced or decreased by vertical mixing. These previous studies clearly showed that vertical mixing within the water column modulates the photosynthetic response to UVBR. Given the strong link between nitrogen assimilation and photosynthesis and the sensitivity of nitrogen uptake to UVBR (*see below*), we hypothesized that the effect of UVB on nitrogen uptake by phytoplankton will also be modulated by vertical mixing.

During a 7-d mesocosm experiment, Fauchot et al. (2000) determined the influence of enhanced UVBR on N utilization by a natural assemblage of phytoplankton enclosed in a mesocosm and submitted to a fast (turnover time of 1 h) mixing regime. They observed only little detrimental effect of enhanced UVBR on the uptake rates of nitrate and ammonium throughout the study. However, enhanced UVBR induced a large reduction in urea uptake during the postbloom period. Because the internal nitrogen pools (internal urea, free amino acids, and proteins) of phytoplankton were not affected by the enhanced UVBR treatments, these authors suggested that phytoplankton were able to photorepair UVBR damage during their transit in the deeper part of the mesocosm. Using a similar experimental design, we examined the influence of two mixing rates on the uptake rate of dissolved inorganic and organic nitrogen by a natural phytoplanktonic community under ambient and enhanced UVBR.

Materials and methods

Experimental procedure—Mesocosm experiments were conducted at the Pointe-au-Père field station on the south shore of the Lower St. Lawrence Estuary (Québec, Canada: 48°31′N, 68°28′W) from 22 to 31 July 1997. Four tanks (depth 2.25 m) of 3,200 liters capacity each were used with two separate polyethylene mesocosms (1,500 liters each) in each tank in order to create replicates of two experimental UVBR and mixing regimes. Experimental water was pumped from the Lower St. Lawrence Estuary (wharf of Ste. Anne-des-Monts, Canada: 49°08′N, 66°29′W) at 2 m depth on 21 July 1997 from 1400 to 1500 h. The seawater was passed through a 202-μm Nitex screen to remove large zooplankton and the eight mesocosms were filled in parallel from 1730 to 2000 h. Plankton communities within the mesocosms were submitted to four different environmental conditions: (1) natural ambient UVBR and fast mixing regime (NAT fast), (2) enhanced UVBR and fast mixing regime (+UVBR fast), (3) natural ambient UVBR and slow mixing regime (NAT slow), and (4) enhanced-UVBR and slow mixing regime (+UVBR slow). The UVB intensities were increased above ambient radiation using two UVB lamps (model XX15B, Spectronics Corporation) with an emission peak at 312 nm, which were turned on from 0900 to 1500 h. The shorter wavelengths not encountered in nature but emitted by lamps were eliminated by covering the lamps with aged 0.13-mm cellulose acetate sheets that were changed daily. The water in each mesocosm was continuously mixed from 15 cm below the surface water to the bottom of the mesocosm using a small pump (Little Giant model 2-MD-HC) with two different flow rates to ensure a turnover of the whole water mass within the mesocosm every 1 h (fast mixing regime) and every 3 h (slow mixing regime). Water temperature in the eight mesocosms was adjusted to the in situ water temperature by circulating local estuarine water through a piping system surrounding each tank. Water removed from the mesocosms for sampling was not replaced. However, the water level in the mesocosms was kept constant relative to the top of the tanks through the addition of water between the tank wall and the polyethylene mesocosms after each sampling. This maintained a constant distance of 40 cm between the water surface in the mesocosms and the UVB lamps throughout the entire experiment. To ensure the same shading effect as the lamps in the natural treatments, two dummy lamps (wooden replicates) were installed over the NAT slow and NAT fast mesocosms. Because of shading created by the tank walls, the lamps, and lamp dummies, only 37% of the incident photosynthetically available radiation (PAR) reached the surface of the mesocosms in the early morning (Belzile et al. 1998). During rain events and nights, polyethylene screens were installed on top of the tanks and removed afterwards.

Water temperature, salinity, and light measurements—The water temperature was measured hourly between the two mesocosms in each tank with thermocouples, type J or type T, connected to a datalogger (21X, Campbell Scientific). In each mesocosm, vertical water temperature profiles were obtained using the temperature sensor of the PUV-500 radiometer (Biospherical Instruments), which also measured irradiance intensity and attenuation in the water column. Salinity was determined with a handheld salinity refractometer (Vista Series Instruments A366ATC) from daily subsamples taken at the surface and at the bottom of the mesocosms. During the experiment, the water temperature in the meso-

cosms varied between 8.2 and 13.7°C, whereas salinity remained relatively constant at 26.

Incident intensities of ambient PAR (400–700 nm), ultraviolet-A radiation (UVAR, 320–400 nm), and UVBR (280–320 nm) were recorded every 5 min with an IL-1700 radiometer (International Light) equipped with SUD033/PAR/QNDS1/W, SUD033/UVA/W, and SUD240/SPS300/T/W broadband and flat sensors. Irradiance throughout the water column was measured with a PUV-500 profiling radiometer, which provided a measure of cosine-corrected downwelling irradiance, at 305, 320, 340, and 380 nm, and PAR. The 305-nm channel was corrected according to the recommendations of Kirk et al. (1994). The apparent attenuation coefficients for the UV wavelengths were calculated using a correction factor (1.19) to consider the geometric conditions of the light field as described by Whitehead et al. (2000). In order to determine the light characteristic of the mesocosms, a preliminary experiment was conducted on 12 July 1997. During this preliminary phase, the UVB lamp emission spectrum and the solar spectrum were measured at noon using Optronic Laboratories OL 754 and OL 752 spectroradiometers, respectively. More details on the experimental setup and the irradiance measurements are given in Belzile et al. (1998), Mostajir et al. (1999*a*), and Whitehead et al. (2000).

Chemical and biological analyses—Water samples were collected from each mesocosm at 0900 h daily, at 0.15 and 2 m below the surface water. For chlorophyll *a* (Chl *a*), subsamples (400 ml) were sized-fractionated in parallel on Whatman GF/F glass fiber filters (total phytoplankton biomass) and Nuclepore polycarbonate membranes with 5 μm nominal pore size (phytoplankton >5 μm biomass). Chl *a* retained on the filters was then determined with a 10-005R Turner Designs fluorometer following a 24-h extraction in 90% acetone at 4°C before and after acidification with 5% HCl (Parsons et al. 1984). Subsamples were also filtered onto Nuclepore polycarbonate 0.8-μm filters using an all-plastic filtration unit, and the filters were frozen at −80°C for later determination of biogenic silica (BiogSi). BiogSi retained on filters was first converted into silicic acid (hydrolysis method of Paasche 1980), which was then measured as described below. Subsamples from 0.15 and 2 m depths on days 1, 5, 7, and 10 were fixed with acidic lugol (Parsons et al. 1984) for later identification and enumeration of phytoplankton >3 μm using the Utermöhl technique (Lund et al. 1958). The abundance of small phytoplankton (1–5 μm) was determined with a FACSORT Analyzer flow cytometer (Becton-Dickinson) fitted with a 488-nm laser using the same protocol described previously by Mostajir et al. (1999*b*).

For nutrient analyses, subsamples were filtered (<10 cm Hg) through precombusted (500°C for 5 h) Whatman GF/F glass fiber filters. Inorganic and organic dissolved nutrients were analyzed in the filtrates. The concentration of ammonium (NH_4^+) was determined immediately using the method of Solórzano (1969) as described by Parsons et al. (1984). The remainder of the filtrate was kept frozen at −80°C for later analysis of nitrate plus nitrite ($NO_3^- + NO_2^-$), nitrite (NO_2^-), phosphate (PO_4^{3-}), and silicic acid ($Si(OH)_4$) using an Alpkem FS III autoanalyzer. Urea was analyzed with the autoanalyzer using the diacethyl monoxime method (Price and Harrison 1987).

Nitrogen transport rates were estimated according to the tracer method of Dugdale and Wilkerson (1986). Trace additions of ^{15}N isotope ($Na^{15}NO_3$, $(^{15}NH_4)_2SO_4$ or ^{15}N-urea) were made to 400-ml subsamples for a final concentration of 0.1 μmol L^{-1} for $^{15}NO_3^-$ and $^{15}NH_4^+$ and of 0.05 μmol L^{-1} for ^{15}N-urea. Saturating enrichments of nitrate were also performed with addition of 0.5 μmol L^{-1} $Na^{15}NO_3$ plus 5 μmol L^{-1} $Na^{14}NO_3$. The inoculated subsamples were incubated in Whirlpak polyethylene bags. The bags were submerged in the center of the mesocosms at their respective sampling depths (0.15 and 2 m). After 4 h of incubation from 1000 to 1400 h (24 h for saturating NO_3^- transport rate: ρNO_3^- sat), the subsamples were filtered onto precombusted Whatman GF/F filters and stored frozen at −80°C. After being dried at 60°C for 24 h, samples were pelletized and analyzed for ^{15}N isotope ratios and particulate organic nitrogen (PON) and carbon (POC) using an Europa Scientific ANCA mass spectrometer. Nitrogen transport rates were calculated using the equation of Dugdale and Wilkerson (1986).

$$\rho_N = \frac{[C_p - C_0]}{[C_d - C_0] \times \Delta t} \times \frac{PON_f}{Vol}$$

C_p is the concentration of the labeled compound (in atom % ^{15}N) in the particulate phase after incubation, C_d is the concentration of the labeled compound (in atom % ^{15}N) in the dissolved phase at time zero, C_0 ($= 0.366\%$) is the natural concentration of the labeled compound (in atom % ^{15}N), Δt is the incubation time, PON_f is the particulate organic nitrogen at the end of the incubation, and Vol is the filtered volume.

The values of nitrate at saturating concentration, ammonium, and urea transport rates were corrected for the isotope dilution effect (Kanda et al. 1987).

Statistical analyses—In order to test for significant differences between the UVBR treatments, mixing regimes, and sampling depths on the various chemical and biological variables, multivariate analyses of variance (MANOVA, Systat v.8.0, SPSS) for repeated measures were performed (von Ende 1993). In this statistical method, the 10 repeated measures of a given variable were considered as 10 dependent variables (von Ende 1993). In this multivariate context, the dependent variables, for example, were the nitrate concentrations on each of the 10 sampling dates, and the treatments were the UVBR regime, the mixing regime, and the sampling depth. Data varied in the same magnitude and were generally normally distributed, as checked by using a normal probability plot and the one-sample Kolmogorov–Smirnov test. The circularity assumption that concerns homogeneity of the variance–covariance matrix was checked using Huynh–Feldt's statistic (Scheiner and Gurevitch 1993). Following the MANOVA results, a one-way analysis of variance and Student's *t*-test were used to test the difference within the various factors on the variables for each sampling day. Significance threshold was set at $p < 0.05$.

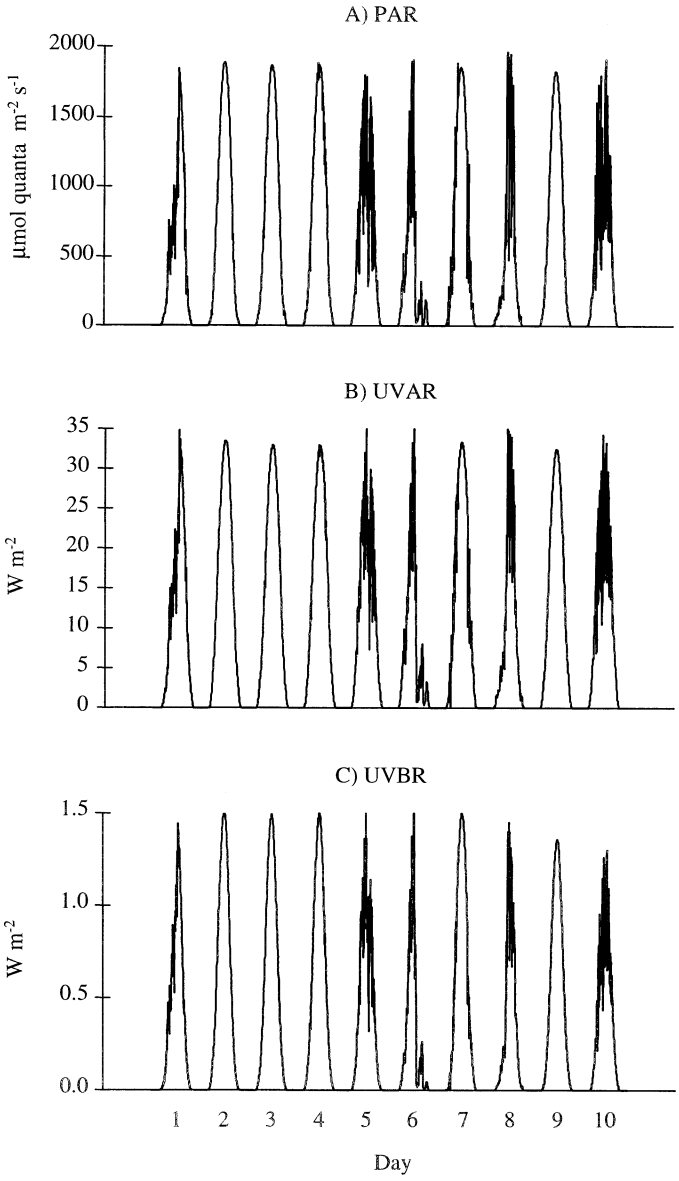

Fig. 1. Temporal variations of incident (A) PAR (400–700 nm), (B) UVAR (320–400 nm), and (C) UVBR (280–320 nm) from day 1 (22 July) to day 10 (31 July 1997) measured at the study site (Pointe-au-Père field station on the south shore of the Lower St. Lawrence Estuary, Québec, Canada: 48°31′N, 68°28′W).

Results

Irradiance—No large difference between days was observed for natural incident irradiance (PAR, UVAR, and UVBR) during the mesocosm experiment (Fig. 1). The average maximal incident PAR, UVAR, and UVBR radiation around noon for the entire study period were 1,859 ± 86 μmol photons m^{-2} s^{-1}, 33.49 ± 2.43 W m^{-2}, and 1.40 ± 0.12 W m^{-2}, respectively. Daily incident PAR, UVAR, and UVBR varied from 24 to 50 mol photons m^{-2}, 499 to 965 kJ m^{-2}, and 19 to 36 kJ m^{-2}, respectively.

The plankton communities within the mesocosms received the same proportion of the daily incident irradiance under the four treatments. The daily incident UVBR dose (natural or enhanced) to which phytoplankton cells were exposed was thus the same in the two mixing regimes. The delivery of the dose was however different, with the exposure time to UVBR (natural and enhanced) during each passage through the surface layer being longer under the slow mixing regime than under the fast mixing regime.

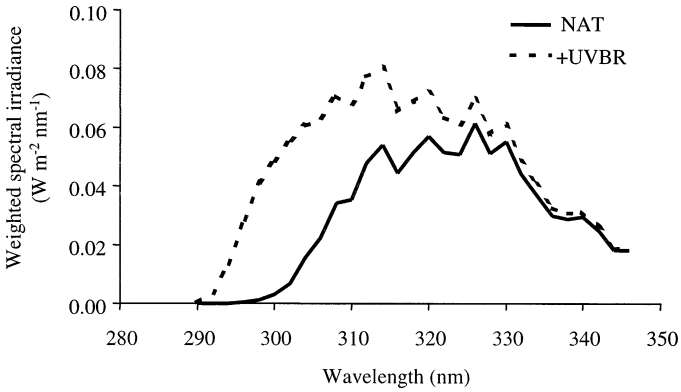

Fig. 2. Weighted spectral irradiances at the water surface of the mesocosms under natural UVBR and enhanced UVBR treatments on 12 July 1997 at 1200 h. The spectral irradiances are weighted by the biological function for ρNH_4^+ inhibition normalized to 1 at 300 nm (Behrenfeld et al. 1995).

UV enhancement provided by the lamps averaged 0.0475, 0.0421, 0.0176, and 0.0008 W m^{-2} nm^{-1} just below the water surface at 305, 320, 340, and 380 nm, respectively. The UV radiation was rapidly attenuated within the mesocosms; the mean depths of 1% of surface irradiance at 305, 320, 340, and 380 nm were 0.98, 1.14, 1.43, and 2.24 m, respectively (Whitehead et al. 2000). On average, 19% of the surface PAR reached the bottom of the mesocosms.

Weighted spectral irradiances measured at the water surface of the mesocosms on the clear sunny day of 12 July 1997 at 1200 h for the two UVBR treatments are presented in Fig. 2. The spectral irradiances between 290 and 347 nm were weighted by the biological weighting function of Behrenfeld et al. (1995) for UV inhibition of the ammonium transport rate (ρNH_4^+). The relative increase in irradiance between 290 and 320 nm, as compared to the natural UVBR treatments, was 122% in the enhanced UVBR treatments. The relative increase was 12% between 320 and 347 nm.

Ambient nutrients—Because MANOVAs with repeated measures showed that there was no significant difference between the sampling depths on the ambient nutrient concentrations, the mean values of the measurements taken at 0.15 and 2 m are presented in Fig. 3. Nutrients exhibited a similar general pattern in all mesocosms with no significant difference between the UVBR treatments and only a slight but sometimes significant difference between the mixing regimes for nitrate, nitrite, ammonium, phosphate, and silicic acid. Nitrate concentrations decreased from ~0.35 μmol L^{-1} on day 1 to the limit of detection on days 5 and 6, then increased to a peak concentration of 0.43 μmol L^{-1} on day 8 (Fig. 3A) because of a nitrification event (*see Discussion*). Nitrite concentrations remained between 0.14 and 0.30 μmol

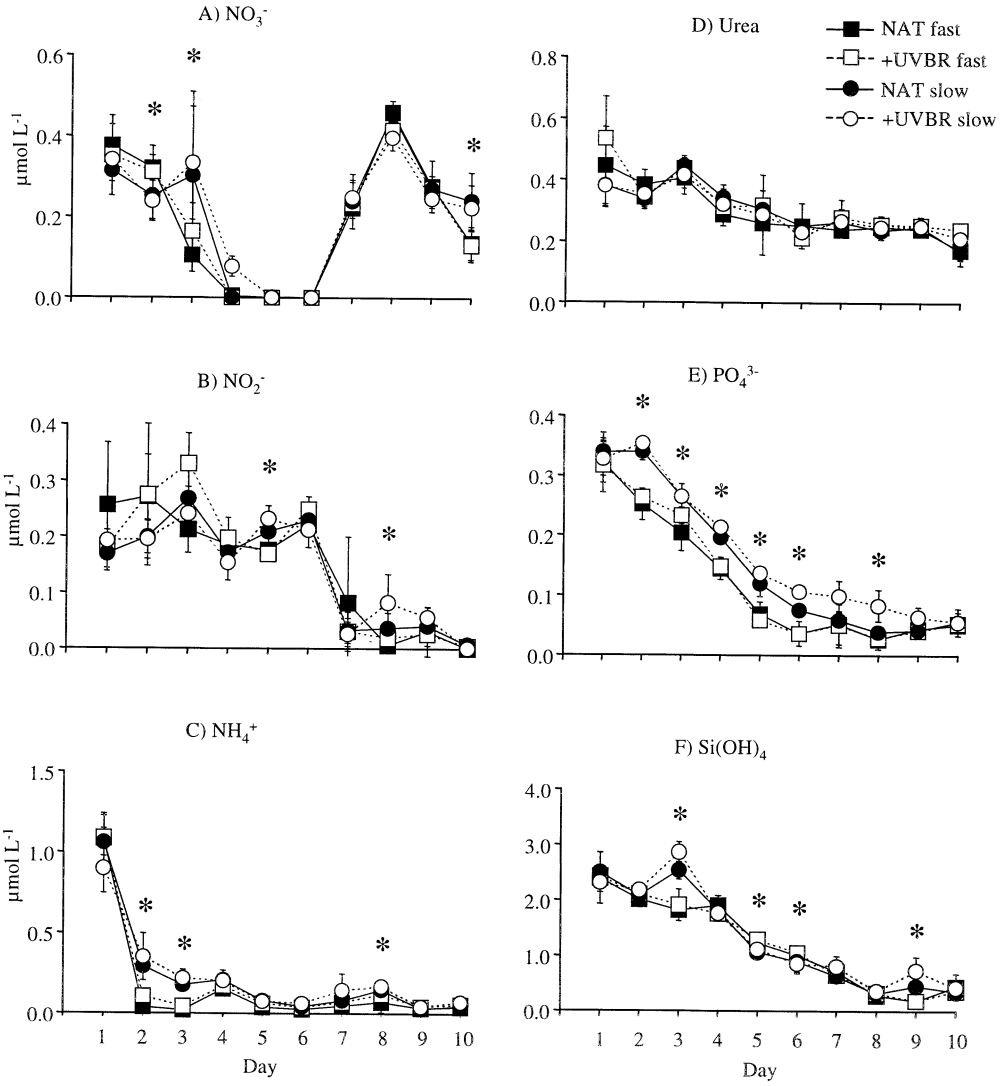

Fig. 3. Temporal variations (average ± SD) of the ambient concentrations of (A) nitrate, (B) nitrite, (C) ammonium, (D) urea, (E) phosphate, and (F) silicic acid in the mesocosms under four experimental treatments: natural ambient incident solar radiation and fast mixing (NAT fast), enhanced UVBR and fast mixing (+UVBR fast), natural ambient incident solar radiation and slow mixing (NAT slow), and enhanced UVBR and slow mixing (+UVBR slow). Asterisks denote a significant difference between the mixing regimes.

L^{-1} from day 1 to day 6 and decreased drastically to 0.04 μmol L^{-1} on day 7 and remained at a low level for the rest of the experiment (Fig. 3B). Ammonium concentrations decreased from 1 μmol L^{-1} on day 1 to <0.4 μmol L^{-1} on day 2 and remained below 0.2 μmol L^{-1} for the rest of the experiment, except for two peaks observed on days 4 and 8 (Fig. 3C). Urea decreased from 0.45 μmol L^{-1} on day 1 to 0.25 μmol L^{-1} on day 6, then stayed relatively constant for the rest of the experiment (Fig. 3D). In contrast with the other nutrients, phosphate and silicic acid concentrations decreased more gradually from 0.33 and 2.5 μmol L^{-1} to 0.05 and 0.4 μmol L^{-1}, respectively, during the experiment (Fig. 3E,F). Significant differences between the two mixing regimes were detected on days 2, 3, and 10 for nitrate; on days 5 and 8 for nitrite; on days 2, 3, and 8 for ammonium; from days 2 to 6 and on day 8 for phosphate; and on four occasions between days 3 and 9 for silicic acid (Fig. 3A–C,E,F). The concentrations of these nutrients were generally slightly higher under the slow mixing regime than under the fast mixing regime, suggesting lower uptake rates.

Phytoplankton biomass and abundance—There was no significant difference between the sampling depths for the plankton biomass (Chl *a*, POC, PON, and BiogSi) and the phytoplankton abundance (Table 1); hence, the mean values are presented in Fig. 4. The two mixing regimes were thus sufficient to maintain a homogeneous vertical distribution of nutrients and particulate matter in the mesocosms. The plankton biomass indices were not affected by the different UVBR treatments. On the other hand, the mixing regimes had a significant effect on Chl *a*, POC, PON, and BiogSi and on phytoplankton abundance (Fig. 4A; Table 1). In the

Table 1. Average (SD) values of the 1–5-μm phytoplankton abundance determined by flow cytometry, diatom abundance determined with the Utermöhl technique, and the percent contribution of phytoplankton cells >5 μm to total Chl *a* biomass in the mesocosms under the fast and slow mixing regimes. Asterisks (*) denote a sampling day when phytoplankton abundance and percent Chl *a* concentration are significantly higher under the fast or the slow mixing regime. nd, not determined.

		Phytoplankton abundance (10^6 cells L^{-1})					
Regime	Day	Cyanobacteria cells	Flagellate cells 1–5 μm	Total diatom cells	*L. minimus*	*S. costatum*	Chl *a* >5 μm (%)
Fast	1	1.26(0.23)	0.45(0.02)	0.13(0.01)	0.02(0.00)	0.02(0.00)	82(8)
	2	0.98(0.15)	0.39(0.05)	nd	nd	nd	93(5)
	3	0.93(0.06)	0.49(0.03)	nd	nd	nd	98(4)*
	4	1.12(0.08)	0.87(0.07)	nd	nd	nd	96(6)*
	5	1.91(0.05)	1.50(0.15)	0.82(0.14)	0.24(0.04)	0.30(0.10)	98(3)*
	6	2.56(0.15)	1.97(0.29)	nd	nd	nd	99(3)*
	7	1.92(0.26)*	2.08(0.09)	4.49(0.52)*	1.11(0.14)	2.65(0.44)*	99(1)*
	8	0.99(0.11)*	1.81(0.38)	nd	nd	nd	99(2)*
	9	0.58(0.06)*	2.11(0.41)	nd	nd	nd	98(2)*
	10	0.92(0.07)*	2.11(0.64)	6.24(0.89)*	1.25(0.47)	4.24(0.56)*	93(5)*
Slow	1	1.14(0.29)	0.40(0.09)	0.13(0.01)	0.02(0.01)	0.02(0.01)	85(7)
	2	1.21(0.15)	0.41(0.05)	nd	nd	nd	88(6)
	3	2.96(0.10)*	0.76(0.05)*	nd	nd	nd	90(7)
	4	5.42(0.28)*	1.37(0.05)*	nd	nd	nd	88(8)
	5	7.59(0.16)*	2.70(0.27)*	1.02(0.16)*	0.29(0.09)	0.30(0.05)	90(6)
	6	4.02(0.64)*	2.79(0.21)*	nd	nd	nd	89(5)
	7	0.99(0.13)	2.74(0.27)*	3.33(0.54)	1.04(0.23)	1.46(0.34)	88(7)
	8	0.35(0.08)	2.70(0.55)*	nd	nd	nd	83(9)
	9	0.42(0.06)	3.00(0.29)*	nd	nd	nd	83(8)
	10	0.63(0.18)	3.22(0.45)*	5.19(0.40)	3.06(0.40)*	1.63(0.34)	70(6)

fast-mixing (NAT and +UVBR) mesocosms, Chl *a* concentrations increased from 0.8 to ~6 μg L^{-1} between day 1 and the end of the experiment (Fig. 4A). In the slow-mixing (NAT and +UVBR) mesocosms, we measured slightly higher Chl *a* concentrations between days 3 and 6, but lower maximum values were reached afterward (~4 μg L^{-1}) (Fig. 4A). POC, PON, and BiogSi also increased during the course of the experiment from 27 to 70 μmol L^{-1} for POC, from 2.5 to 5.7 μmol L^{-1} for PON, and from 1.5 to 3.4 μmol L^{-1} for BiogSi (Fig. 4B–D). As observed for Chl *a*, lower POC, PON, and BiogSi concentrations were measured in the slow-mixing (NAT and +UVBR) mesocosms than in the fast-mixing (NAT and +UVBR) mesocosms during the last 3 d of the experiment (Fig. 4B–D).

The general increase in phytoplankton biomass observed in all mesocosms resulted from the accumulation of both small cells (between 1 and 5 μm; mainly cyanobacteria and small eukaryotic cells) and centric diatoms (Table 1). Cells larger than 5 μm always contributed >70% of the total Chl *a* biomass and up to 99% on some sampling days (Table 1). The phytoplankton biomass was thus dominated by large diatom cells in all mesocosms. At the beginning of the experiment, the diatom community was dominated by *Skeletonema costatum*, *Leptocylindrus minimus*, and *Chaetoceros furcellatus*. The abundance of diatoms increased progressively during the first 5 d and more abruptly between days 5 and 7 in all mesocosms (Table 1). As observed for most of the biomass indices measured, the total abundance of diatoms was significantly lower in the slow-mixing (NAT and +UVBR) mesocosms than in the fast-mixing (NAT and +UVBR) mesocosms during the last days of the experiment. In addition, the mixing regimes influenced the composition of the diatom assemblage, with *L. minimus* and *S. costatum* dominating the community under the slow and fast mixing regimes, respectively. In all mesocosms, cyanobacteria dominated the total 1–5 μm phytoplankton abundance during the first 6 d of the experiment, whereas small eukaryotic cells (mainly prymnesiophytes) dominated during the rest of the experiment, especially under the slow mixing regime (Table 1). Thus, the reduction of the mixing rate resulted in a decrease of the phytoplankton biomass and an increase in the relative abundance of *L. minimus* and prymnesiophytes in the assemblage. On the other hand, changes in UVBR regimes did not affect the plankton biomass or the phytoplankton abundance.

Nitrogen transport rates—As observed for other variables presented above, we generally found no statistically significant difference between the nitrogen uptake rates (trace addition) measured at the two sampling depths for both mixing regimes. Although not significant, the uptake rates of the three nitrogenous nutrients for both mixing regimes tended to be higher at 0.15 m than at 2 m in the mesocosms under ambient UVBR, whereas they tended to be higher at the bottom than at the surface under enhanced UVBR conditions. Because this trend was not pronounced enough to be significant, the direct effects of UVBR on N uptake during the 4-h incubations were too small to be detected, confounded with the effects of reduced PAR (i.e., rates were depressed by UVBR at the surface and by low PAR at the bottom so that peak rates might have been at some intermediate depth), or both. However, as mentioned below, sig-

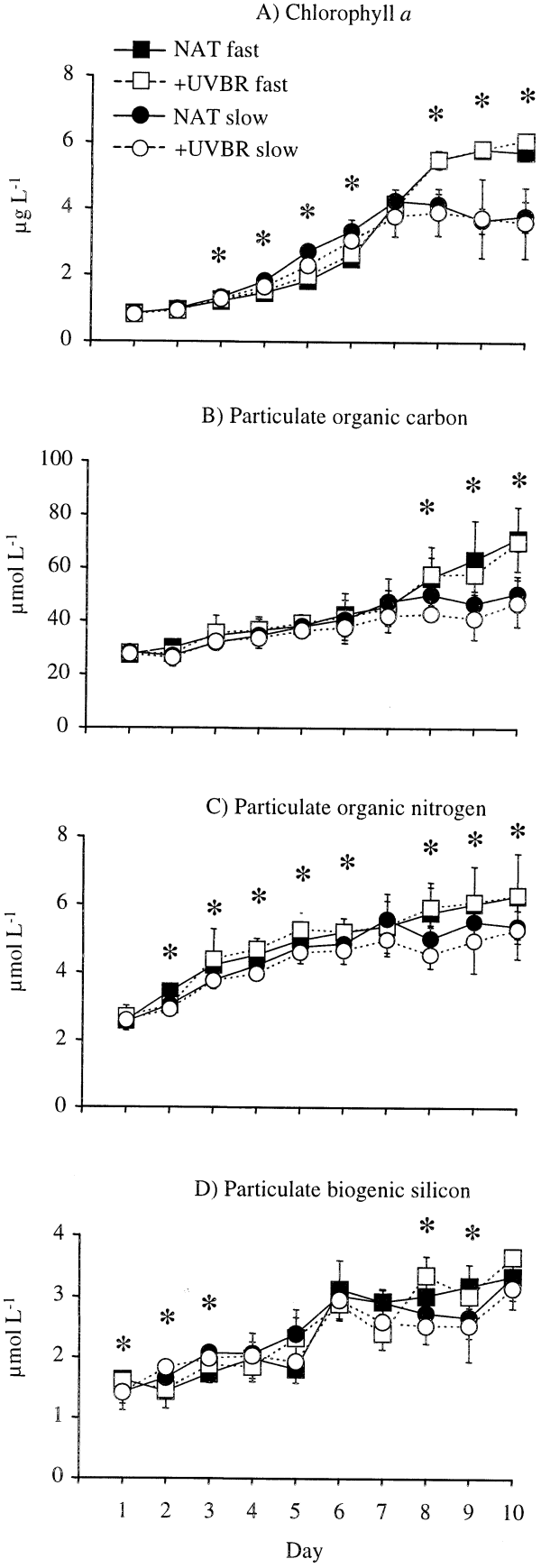

nificant differences in nitrogen uptake rates between ambient and enhanced UVBR conditions were observed under the slow mixing regime at both the surface and the bottom of the mesocosms (Fig. 5A,C,F). This indicates that the phytoplankton assemblage, which developed under the slow mixing regime, was more sensitive to UVBR enhancement than the one growing under the fast mixing regime.

A similar general pattern of nitrogen transport rates was observed in all mesocosms, although both the mixing regimes and the UVBR treatments occasionally affected these rates (Fig. 5). In all mesocosms, nitrate transport rates increased slowly from <0.001 μmol L^{-1} h^{-1} to 0.013 μmol L^{-1} h^{-1} during the first 6 d, then more abruptly on day 7 to reach a maximum value of 0.09 μmol L^{-1} h^{-1} on day 8 (Fig. 5A). Nitrate transport rates then decreased to reach 0.04 μmol L^{-1} h^{-1} on day 10 (Fig. 5A). We started to detect the influence of the mixing regimes only on day 6 (and subsequently on days 8 and 9) with significantly lower nitrate transport rates measured in the slow-mixing (NAT and +UVBR) mesocosms as compared to the fast-mixing (NAT and +UVBR) mesocosms. In addition, a significant difference between UVBR treatments was observed on days 7 and 8 with lower nitrate transport rates in the +UVBR slow-mixing mesocosms than in the NAT slow-mixing mesocosms. As it can be seen in Fig. 5D, the difference between UVBR treatments was no longer significant when the nitrate transport rates were normalized to the Chl *a* biomass present in each mesocosm, indicating that the difference between the UVBR treatments resulted from changes in biomass rather than in cellular physiology. However, the difference between mixing regimes was still detectable on day 6 and especially on day 10 when the ρNO_3^- : Chl *a* ratios were lower under the fast mixing regime than under the slow mixing regime.

Ammonium transport rates were generally lower than 0.02 μmol L^{-1} h^{-1} during the first 3 d of the experiment, increased up to $\sim$0.07 μmol L^{-1} h^{-1} on day 4, and remained between $\sim$0.03 and 0.06 μmol L^{-1} h^{-1} for the rest of the experiment (Fig. 5B). A significant difference between the mixing regimes was detected on day 4 with lower transport rates under the slow (NAT and +UVBR) than under the fast (NAT and +UVBR) mixing regimes. When normalized to Chl *a*, a generally small but significant difference between mixing regimes was observed from day 3 to day 6 and on days 8 and 10 (Fig. 5E). The influence of the mixing regimes on the ρNH_4^+ : Chl *a* ratio was more pronounced on day 4, with lower Chl *a*–specific ammonium transport rates measured in the slow (NAT and +UVBR) than in the fast (NAT and +UVBR) mixing mesocosms.

Urea transport rates were negligible at the beginning of the experiment in all mesocosms, increased gradually up to $\sim$0.02 μmol L^{-1} h^{-1} between days 3 and 6, and remained between $\sim$0.01 and 0.015 μmol L^{-1} h^{-1} for the rest of the

←

Fig. 4. Temporal variations of the concentrations of (A) Chl *a*, (B) POC, (C) PON, and (D) biogenic silica in the mesocosms under four experimental treatments (*see Fig. 3 for details*). Asterisks denote a significant difference between the mixing regimes.

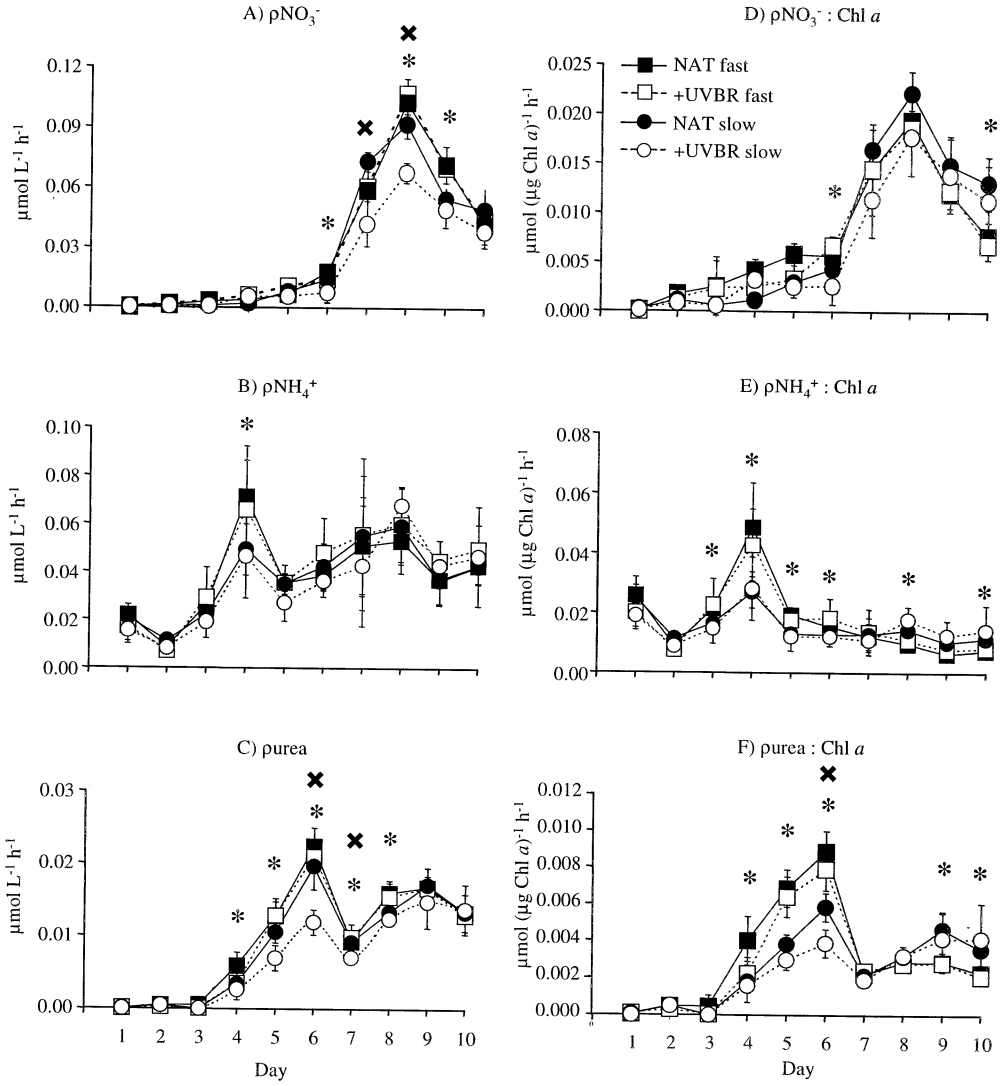

Fig. 5. Temporal variations of (A, B, and C) transport rates (ρN) and (D, E, and F) Chl *a*–specific transport rates (ρN : Chl *a*) of nitrate, ammonium and urea in the mesocosms under four experimental treatments (*see Fig. 3 for details*). Asterisks denote a significant difference between the mixing regimes, whereas crosses express a significant difference between the natural and enhanced UVBR treatments under the slow mixing regime.

experiment (Fig. 5C). A significant difference between the mixing regimes was detected from days 4 to 8, with urea transport rates being lower in the slow-mixing (NAT and +UVBR) mesocosms than in the fast-mixing (NAT and +UVBR) mesocosms. The UVBR treatments also affected the urea transport rates, but only on days 6 and 7, with lower values in +UVBR slow-mixing mesocosms than in the NAT slow-mixing mesocosms. The urea transport rates normalized to Chl *a* exhibited a similar temporal pattern with minimum values at the beginning, maximum values in the middle of the experiment, and intermediate values during the rest of the sampling period (Fig. 5F). Both treatments (mixing regimes and UVBR treatments) affected these biomass-normalized rates, suggesting a physiological response of the phytoplankton assemblage to these stresses. On day 4, ρurea : Chl *a* values were lower in the NAT slow-mixing mesocosms than in the NAT fast-mixing mesocosms. The difference between mixing regimes was maximum on days 5 and 6 with ρurea : Chl *a* values being consistently lower (by up to 50%) in the slow (NAT and +UVBR) than in the fast (NAT and +UVBR) mixing mesocosms. Interestingly, this pattern was reversed on days 9 and 10 when lower Chl *a*–specific urea transport rates were measured in the fast-mixing (NAT and +UVBR) than in the slow-mixing (NAT and +UVBR) mesocosms. The different phytoplankton assemblages present in the mesocosms toward the end of the sampling with different mixing regimes seem to have different urea uptake characteristics. The UVBR regime also significantly affected the Chl *a*–specific urea transport rate, but only on day 6 when lower rates were measured in the +UVBR slow-mixing mesocosms than in the NAT slow-mixing mesocosms.

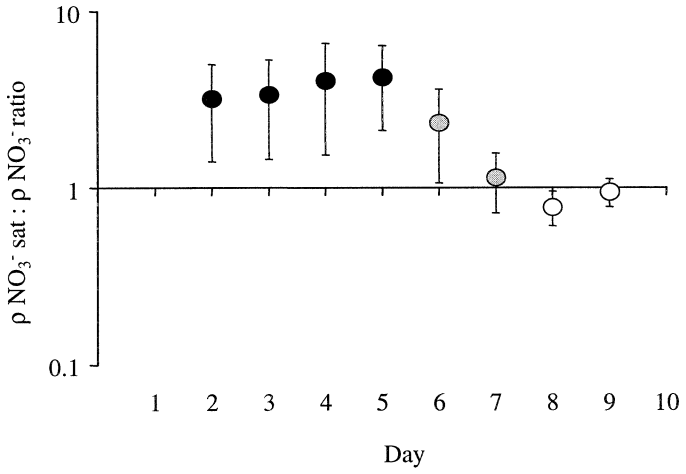

Fig. 6. Temporal variation in the ratio of nitrate transport rate at saturating concentration to nitrate transport rate at trace concentration for all mesocosms (average ± SD).

Discussion

Nutrients and phytoplankton dynamics in all mesocosms—Nutrient concentrations were low at the beginning of the experiment (NO_3^- = 0.35 μmol L^{-1}, NH_4^+ = 1 μmol L^{-1}, urea = 0.45 μmol L^{-1}, and $Si(OH)_4$ = 2.5 μmol L^{-1}), as typically measured in the Lower St. Lawrence Estuary in summer (Tremblay et al. 2000), and decreased rapidly to reach undetectable concentrations for nitrate, nitrite, and ammonium (Fig. 3A–C). Concurrent with the decrease in nutrients, an increase in Chl *a*, POC, PON, and BiogSi was observed in all treatments, coinciding with the development of a diatom community dominated by *S. costatum* and *L. minimus* (Fig. 4). The nitrate concentrations were likely inadequate to satisfy the nitrate demand of the phytoplankton community during the first 6 d, as shown from the ratio of the transport rate of nitrate at saturating concentration to the transport rate of nitrate at trace concentration (ρNO_3^- sat: ρNO_3^-) (Glibert and McCarthy 1984), which was >1 from day 2 to day 6 in all treatments (Fig. 6). Despite the nitrate limitation, the phytoplankton biomass increased slightly between day 1 and day 6 in all mesocosms. The increases in transport and Chl *a*–specific transport rates of ammonium and urea measured between days 4 and 6 indicate that the phytoplankton assemblages shifted toward these other nitrogen sources to fulfill their N requirement in all mesocosms.

The nitrate concentrations increased suddenly on days 7 and 8 (Fig. 3A). This increase coincided with a significant decrease in nitrite concentrations in all mesocosms (Fig. 3B), suggesting a bacterial nitrification event. Several factors control the activity of nitrifying bacteria in marine environments (*reviewed in* Kaplan 1983). These include the concentrations of ammonium, nitrite, and organic matter as substrates for marine-nitrifying bacteria. In the mesocosms, the growth of nitrifying bacteria might have been stimulated by the accumulation of particulate matter. The mean number of copepod fecal pellets increased from 186 L^{-1} to 655 L^{-1} between days 1 and 5 in all mesocosms and remained >300 L^{-1} until the end of the experiment (B. Mostajir unpubl. data). These fecal pellets can provide suitable adsorption sites for nitrifying bacteria and stimulate their growth. Between days 5 and 7, the concentration of free living bacteria decreased from ~2 × 10^9 cells L^{-1} to ~1 × 10^9 cells L^{-1} in all mesocosms, presumably because of lysis, bacterivory, or both (Whitehead et al. 2000). The decrease in the abundance of bacteria also coincided with a small but significant increase in dissolved organic carbon (DOC) in all mesocosms on day 7 (Whitehead et al. 2000). The remaining heterotrophic bacteria could have remineralized this substrate into NH_4^+. Microzooplankton grazing on bacteria also could have favored the release of NH_4^+. The available dissolved nitrogen sources (i.e., NO_2^-, NH_4^+, and dissolved organic nitrogen) were probably rapidly consumed and transformed into NO_3^- by nitrifying bacteria during the nighttime, as indicated by the large increase in NO_3^- on days 7 and 8 in all treatments. This increase in nitrate stimulated diatom growth, which became more abundant after day 5 in all mesocosms (Table 1). The ρNO_3^- sat: ρNO_3^- ratio decreased to ~1 on day 7 and remained at this level for the rest of the experiment in all mesocosms (Fig. 6), suggesting that the nitrate uptake rates were no longer limited by the ambient nitrate levels. This unexpected nitrate production in all mesocosms after the first 6 d of the experiment shows the potential importance of nitrification within the euphotic zone in the St. Lawrence and provides support to a recent pelagic ecosystem model for the Gulf of St. Lawrence suggesting that 11% of nitrate-based phytoplankton production could originate from in situ recycling (Tian et al. 2000). Ward et al. (1989), Gentilhomme and Raimbault (1994), and Diaz and Raimbault (2000) have already reported that nitrification in the euphotic zone might represent a significant source of nitrate for phytoplankton production.

The shift from ammonium to urea and nitrate uptake observed in all mesocosms, which followed the availability of the nitrogen sources, was previously observed in the Estuary and the Gulf of St. Lawrence (Tremblay et al. 2000). This shift could explain the change in the <5-μm phytoplankton species composition from cyanobacteria to autotrophic flagellates after day 6 in the experiment. The low nutrient availability measured during the first 6 d of this study favored the cyanobacteria, which could be less affected by limited nutrient diffusion than autotrophic flagellates with larger cell volume. Indeed, the cyanobacteria cell number decreased from day 7, whereas the small flagellate cell number remained relatively constant during the last days of the experiment (Table 1). This change in the small phytoplanktonic species composition could be related to the fact that eukaryotic and prokaryotic phytoplankton are generally favored under high and low nutrient concentrations, respectively, as observed in the Gulf of St. Lawrence (Tamigneaux et al. 1995).

At the end of the experiment, nitrate uptake rates decreased in all treatments (Fig. 5A,D), probably because of silicic acid limitation of diatom growth. During this period, phosphorus limitation is unlikely because the atomic ratio of TDN to PO_4^{3-} ranged from 10 to 20, or close to the Redfield value of 16 (Redfield et al. 1963). Moreover, silicic acid concentrations during the last 3 d of the experiment were lower than the range of reported values for the affinity con-

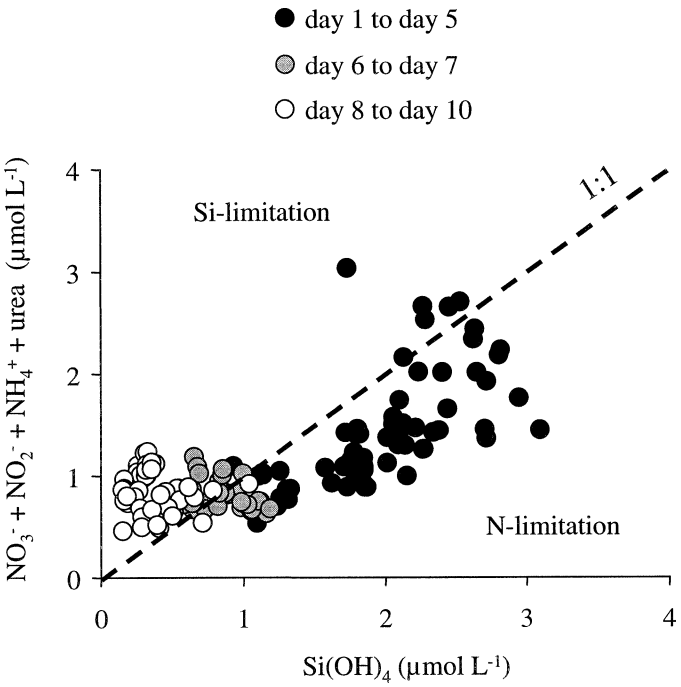

Fig. 7. Concentrations of total dissolved nitrogen (TDN = nitrate + nitrite + ammonium + urea) plotted against the concentrations of silicic acid in all mesocosms for the first 5 d (days 1–5), days 6 and 7, and the last 3 d (days 8–10) of the experiment. The dashed line is the 1 : 1 slope of Brzezinski (1985).

stant of diatoms for silicic acid (K_s = 0.8 to 3 μmol L^{-1}, Conway and Harrison 1977; Nelson et al. 1981).

The temporal change in the availability of the nutrients for phytoplankton growth in the mesocosms can be seen in Fig. 7. The concentrations of TDN plotted against the concentrations of silicic acid in all treatments were compared to the atomic N : Si ratio, which is ~1 : 1 for nutrient-sufficient marine diatoms (Brzezinski 1985). The ratio of TDN to $Si(OH)_4$ was generally <1 from days 1 to 5 for all treatments, showing that nitrogen was the potential limiting nutrient during this period. Despite low ambient nutrient concentrations, the TDN : $Si(OH)_4$ ratio was close to the atomic ratio for nutrient-sufficient marine diatoms on days 6 and 7 in all treatments. The TDN : $Si(OH)_4$ ratio was >1 during the last 3 d of the experiment, indicating that silicic acid was the potential limiting nutrient for diatoms from days 8 to 10 in all treatments.

The pulse in nitrate observed in our mesocosms provides a unique opportunity to study how the release of nitrate limitation leading to silicic acid exhaustion can influence the N transport rate in this system. This is particularly relevant because quasi-simultaneous exhaustion of dissolved inorganic nitrogen and silicic acid have been observed in many oceanic and coastal regions (Zentara and Kamykowski 1981; Sommer 1986), including the St. Lawrence Estuary in the summer (Levasseur and Therriault 1987; Levasseur et al. 1990).

Influence of the mixing regime on the phytoplankton assemblage—The mixing regime had a profound effect on the composition of the phytoplankton assemblage, irrespective of the light regime. As expected, the phytoplankton assemblage was similar in all mesocosms at the beginning of the experiment, but slightly higher concentrations of Chl *a* and lower concentrations of PON soon started to be measured under the slow mixing regime (NAT and +UVBR) than under the fast mixing regime (NAT and +UVBR) during the first 6 d of the experiment (prenitrate pulse period; Fig. 4A,C). During this period, cyanobacteria and flagellate cells were more numerous under the slow mixing regime than under the fast regime, which could partly explain the variations in the biomass indices. The mixing regime–induced changes in the phytoplankton assemblage became more obvious after the nitrate pulse (day 8 on), with lower biomass (Chl *a*, POC, PON, and BiogSi) consistently measured under the slow mixing regime. This difference in biomass reflected a shift in the composition of the phytoplankton assemblage, with *S. costatum* and *L. minimus* dominating under the fast and slow mixing regime, respectively (Table 1). In addition, the prymnesiophytes were also more abundant under the slow mixing regime. It is interesting to note that although the two mixing rates were both vigorous enough to vertically homogenize the water column of the mesocosms, our low mixing regime favors the accumulation of flagellates, as predicted by Margalef's mandala (Margalef 1978; Margalef et al. 1979). These turbulence-induced changes in the structure of the phytoplankton assemblage, particularly after day 7, turned out to be important, since our results show that each assemblage has a different sensitivity to UVBR. The influence of the light regimes on nutrient dynamics will thus be discussed separately for the two mixing regimes (and associated phytoplankton assemblage).

Phytoplankton nitrogen metabolism under enhanced UVBR and the fast mixing regime—The enhanced UVBR treatments tested in this experiment were somewhat greater than the relative enhancement associated with the ozone hole over Antarctica (1.24-fold in Cullen and Neale [1997] vs. 1.51-fold in our study based on the biological weighting function of Cullen et al. [1992] for inhibition of photosynthesis). The attenuation of PAR and UV wavelengths in the mesocosms was greater than that observed in the Estuary and Gulf of St. Lawrence (Whitehead et al. 2000). At 2 m depth near the bottom of the mesocosms, plankton cells received only 0.008, 0.03, 0.16, and 1.6% of the surface UVR at 305, 320, 340, and 380 nm, respectively, and 19% of the surface PAR. The light regime in the mesocosms was thus comparable to that encountered by phytoplankton cells in situ, but somewhat vertically compressed. No significant differences between sampling depths were detected for the chemical and biological variables, suggesting that the timescale for the examined chemical and biological responses was longer than that for vertical mixing (Lewis et al. 1984).

Under the fast mixing regime, we observed no significant effect of enhanced UVBR treatments on the N uptake rates measured near the surface and at the bottom of the mesocosms. This contrasts with the results from Fauchot et al. (2000) showing a significant reduction in the specific uptake rates of nitrate, ammonium, and urea for samples incubated close to the surface in midsummer under a similar mixing

regime (fast) but a higher UVBR enhancement. This direct UVBR effect was measured during a postdiatom bloom when dissolved nitrogen and silicic acid concentrations were low (~1 μmol L^{-1} and 1–2 μmol L^{-1}, respectively). Their mesocosms were submitted to an increase in UVBR (290–320 nm) of 173% during 8.5 h d^{-1}, compared with 122% for 6 h d^{-1} during the present study. Therefore, the lower level of UVBR and shorter exposure time can explain the lack of response observed during the present study. The phytoplankton community was also different during the Fauchot et al. (2000) experiment. In their study, the decrease in the N uptake rates under enhanced UVBR treatments coincided with a shift in the phytoplankton community from diatom-dominated to a community dominated by naked flagellates and dinoflagellates (Mostajir et al. 1999*b*; Fauchot et al. 2000). In addition, the stress induced by UVBR enhancement on diatom growth appears to have been strong enough to prevent the consumption of silicic acid during the last 2 d of their experiment (Mousseau et al. 2000). The main diatom species were *Chaetoceros debilis, Chaetoceros* spp., and *Thalassiosira* spp. (Mostajir et al. 1999*b*; Fauchot et al. 2000), whereas *S. costatum, L. minimus,* and *C. furcellatus* dominated in the present study. Species-specific variations in sensitivity to UVBR thus also could have contributed to the different response measured during the two investigations.

During long-term experiments (7–14 d) in the laboratory, Behrenfeld et al. (1994) demonstrated that the effect of nutrient limitation on the growth of the marine diatom *Phaeodactylum tricornutum* might exceed the potential inhibitory effect of UVBR. This contrasts with results from short-term UVBR exposure experiments (0.5–4 h) showing potential additive effects between UVBR and nutrient limitation on marine diatoms (Cullen and Lesser 1991; Lesser et al. 1994). The absence of signs of UVBR inhibition on N uptake during our study under the fast mixing regime could indicate that the phytoplankton assemblage was already nutrient-stressed because of the high biomass (and high nutrient demand) and low dissolved nitrogen and silicic acid concentrations. Under these circumstances, our results suggest that the addition of another stress (UVBR in that case) might have no effect.

Phytoplankton nitrogen metabolism under enhanced UVBR and the slow mixing regime—The reduction of the mixing rate of the mesocosms increased the sensitivity of the N transport rates of the phytoplankton assemblages to UVBR enhancement. The nitrate transport rate was significantly lower in the +UVBR slow mesocosms than in the NAT slow mesocosms on days 7 and 8 (Fig. 5A), but this difference disappeared when the rates were normalized by the Chl *a* biomass (Fig. 5D). We thus can conclude that the enhanced UVBR regime had no physiological effect on nitrate transport during the present experiment, even under the slow mixing regime. The urea transport rate also was significantly lower in the +UVBR than in the NAT slow mesocosms on days 6 and 7, but in contrast with nitrate, the difference persisted when the rates were normalized by Chl *a* on day 6 (Fig. 5F). This is the only occasion in our entire data set when a physiological UVBR effect on nitrogen uptake was demonstrated. This clearly shows that the phytoplankton assemblages in the mesocosms were highly resilient to UVBR stress.

In spite of the modest effect observed, our results suggest that the phytoplankton assemblage favored by the slow mixing regime was more sensitive to enhanced UVBR. Species-specific differences in the sensitivity of N uptake/assimilation of phytoplankton to UVBR have been previously reported (Döhler 1990; Döhler and Hagmeier 1997). However, enhanced UVBR reduced N uptake at both the surface and the bottom of the slow mixed mesocosms, suggesting that indirect effects dominated the community responses to UVBR treatments instead of direct effects, like those described by Döhler (1990), Behrenfeld et al. (1995), and Fauchot et al. (2000). In the present study, the difference between UVBR treatments must be caused by long-term (several days) effects of UVBR exposure which mixing distributes over the mesocosm as a whole. These long-term effects might be expressed by changes in phytoplankton species composition or in general physiological state of consumers of dissolved nitrogen (i.e., phytoplankton and presumably bacteria), of producers of dissolved nitrogen (especially the nitrifying bacteria which are sensitive to ambient irradiance), or both. Therefore, there are multiple ways through which the planktonic N dynamics can be affected by UVBR enhancements besides direct effects on the N uptake/assimilation of phytoplankton.

Several previous studies conducted in mesocosms submitted to various mixing rates have shown a lack or only a slight direct effect of enhanced UVBR on the natural phytoplankton community. Forster and Schubert (2001) observed no effect from an increase of ~200% of the natural UVBR on the photosynthetic performance and biomass (Chl *a*) of a summer phytoplankton community dominated by cyanobacteria and small chlorophytes in a well-mixed mesocosm (turnover rate of ~2 h) under low nutrient conditions. Similarly, Wängberg et al. (1999) reported a weak inhibitory effect from an increase of 150–250% of the natural UVBR on the photosynthetic activity and allocation of photosynthate during an 8-d mesocosm study with a mixed summer phytoplankton assemblage under low dissolved inorganic nitrogen concentrations (0.8–1.25 μmol L^{-1}). Keller et al. (1997) also reported no effect from an increase of 200% of the natural UVBR on the abundance of a winter–spring phytoplankton community dominated by the centric diatoms *Thalassiosira* spp. and *Detonula confervaceae* at the beginning of a 3-month well-mixed mesocosm study. Nevertheless, these authors reported significantly lower in vivo fluorescence values under the enhanced UVBR treatments later during the experiment when the community became dominated by *Chaetoceros* spp., *Dinobryon* spp., *L. minimus,* and small flagellates. Therefore, an increase of UVBR does not necessarily induce a major inhibitory effect on the development of the phytoplankton assemblage in a well-mixed environment, in accordance with these previous studies and the present investigation.

Our results suggest that in the St. Lawrence, a reduction in mixing rates results in a shift in the dominant diatom species (from *S. costatum* to *L. minimus*) and an increase in the relative abundance of flagellates. Urea metabolism in this

new phytoplankton assemblage appears to be slightly more sensitive to UVBR. Overall, our results show that the nitrogen metabolism of the St. Lawrence phytoplankton assemblages is remarkably resilient to UVBR stress.

References

BEHRENFELD, M. J., H. LEE II, AND L. F. SMALL. 1994. Interactions between nutritional status and long-term responses to ultraviolet-B radiation stress in a marine diatom. Mar. Biol. **118:** 523–530.

———, D. R. S. LEAN, AND L. LEE. 1995. Ultraviolet-B radiation effects on inorganic nitrogen uptake by natural assemblages of oceanic plankton. J. Phycol. **31:** 25–36.

BELZILE, C., AND OTHERS. 1998. An experimental tool to study the effects of ultraviolet radiation on planktonic communities: A mesocosm approach. Environ. Technol. **19:** 667–682.

BRZEZINSKI, M. A. 1985. The Si:C:N ratio of marine diatoms: Interspecific variability and the effect of some environmental variables. J. Phycol. **21:** 347–357.

CONWAY, H. L., AND P. J. HARRISON. 1977. Marine diatoms grown in chemostats under silicate or ammonium limitation. IV. Transient response of *Chaetoceros debilis, Skeletonema costatum* and *Thalassiosira gravida* to a single addition of a limiting nutrient. Mar. Biol. **43:** 33–43.

CULLEN, J. J., AND M. P. LESSER. 1991. Inhibition of photosynthesis by ultraviolet radiation as a function of dose and dosage rate: Results for a marine diatom. Mar. Biol. **111:** 183–190.

———, AND M. R. LEWIS. 1988. The kinetics of algal photoadaptation in the context of vertical mixing. J. Plankton Res. **10:** 1039–1063.

———, AND P. J. NEALE. 1997. Biological weighting function for describing the effects of ultraviolet radiation on aquatic systems, p. 97–118. *In* D.-P. Häder [ed.], The effects of ozone depletion on aquatic ecosystems. Landes.

———, ———, AND M. P. LESSER. 1992. Biological weighting function for the inhibition of phytoplankton photosynthesis by ultraviolet radiation. Science **258:** 646–650.

DIAZ, F., AND P. RAIMBAULT. 2000. Nitrogen regeneration and dissolved organic nitrogen release during spring in a NW Mediterranean coastal zone (Gulf of Lions): Implications for the estimation of new production. Mar. Ecol. Prog. Ser. **197:** 51–65.

DÖHLER, G. 1985. Effect of UV-B radiation (290–320 nm) on the nitrogen metabolism of several marine diatoms. J. Plant Physiol. **118:** 391–400.

———. 1990. Effect of UV-B (290–320 nm) radiation on uptake of ^{15}N-nitrate by marine diatoms, p. 349–354. *In* W. R. Ullrich, C. Rigano, A. Fuggi, and P. J. Aparicio [eds.], Inorganic nitrogen in plants and microorganisms. Uptake and metabolism. Springer-Verlag.

———, AND E. HAGMEIER. 1997. UV effects on pigments and assimilation of ^{15}N-ammonium and ^{15}N-nitrate by natural marine phytoplankton of the North Sea. Bot. Acta **110:** 481–488.

DUGDALE, R. C., AND F. P. WILKERSON. 1986. The use of ^{15}N to measure nitrogen uptake in eutrophic oceans: Experimental considerations. Limnol. Oceanogr. **31:** 673–689.

FAUCHOT, J., AND OTHERS. 2000. Influence of UV-B radiation on nitrogen utilization by a natural assemblage of phytoplankton. J. Phycol. **36:** 484–496.

FORSTER, R. M., AND H. SCHUBERT. 2001. The effects of ultraviolet radiation on the planktonic community of a shallow, eutrophic estuary: Result of mesocosm experiments. Helgol. Mar. Res. **55:** 23–34.

FURGAL, J. A., AND R. E. H. SMITH. 1997. Ultraviolet radiation and photosynthesis by Georgian Bay phytoplankton of varying nutrient and photoadaptative status. Can. J. Fish. Aquat. Sci. **54:** 1659–1667.

———, W. D. TAYLOR, AND R. E. H. SMITH. 1998. Environmental control of photosynthetate allocation in the phytoplankton of Georgian Bay (Lake Huron). Can. J. Fish. Aquat. Sci. **55:** 726–736.

GENTILHOMME, V., AND P. RAIMBAULT. 1994. Absorption et régénération de l'azote dans la zone frontale du courant algérien (Méditerrannée Occidentale): réévaluation de la production nouvelle. Oceanol. Acta **17:** 555–562.

GLIBERT, P. M., AND J. J. MCCARTHY. 1984. Uptake and assimilation of ammonium and nitrate by phytoplankton: Indices of nutritional status for natural assemblages. J. Plankton Res. **6:** 677–697.

HELBLING, E. W., V. VILLAFAÑE, AND O. HOLM-HANSEN. 1994. Effects of ultraviolet radiation on Antarctic marine phytoplankton photosynthesis with particular attention to the influence of mixing, p. 207–227. *In* C. S. Weiler and P. A. Penhale [eds.], Ultraviolet radiation in Antarctica: Measurements and biological effects. American Geophysical Union.

JEFFREY, W. H., R. PLEDGER, P. AAS, S. HAGER, R. B. COFFIN, R. VON HAVEN, AND D. L. MITCHELL. 1996. Diel and depth profiles of DNA photodamage in bacterioplankton exposed to ambient solar ultraviolet radiation. Mar. Ecol. Prog. Ser. **137:** 283–291.

KANDA, J., E. A. LAWS, T. SAINO, AND A. HATTORI. 1987. An evaluation of isotope dilution effect from conventional data sets of ^{15}N uptake experiments. J. Plankton Res. **9:** 79–90.

KAPLAN, W. A. 1983. Nitrification, p. 139–190. *In* J. E. Carpenter and D. G. Capone [eds.], Nitrogen in the marine environment. Academic Press.

KELLER, A., P. HARGRAVES, H. JEON, G. KLEIN-MACPHEE, E. KLOS, C. OVIATT, AND J. ZHANG. 1997. Ultraviolet-B radiation enhancement does not affect marine trophic levels during a winter–spring bloom. Ecoscience **4:** 129–139.

KERR, J. B., AND C. T. MCELROY. 1993. Evidence for large upward trends of ultraviolet-B radiation linked to ozone depletion. Science **262:** 1032–1034.

KIRK, J. T. O., AND OTHERS. 1994. Measurements of UV-B radiation in two freshwater lakes: An instrument comparison. Arch. Hydrobiol. Beih. Ergeb. Limnol. **43:** 71–99.

LESSER, M. P., J. J. CULLEN, AND P. J. NEALE. 1994. Carbon uptake in a marine diatom during acute exposure to ultraviolet-B radiation: Relative importance of damage and repair. J. Phycol. **30:** 183–192.

LEVASSEUR, M., AND J.-C. THERRIAULT. 1987. Phytoplankton biomass and nutrient dynamics in a tidally induced upwelling: The role of the NO_3:SiO_4 ratio. Mar. Ecol. Prog. Ser. **39:** 87–97.

———, P. J. HARRISON, B. R. HEIMDAL, AND J.-C. THERRIAULT. 1990. Simultaneous nitrogen and silicate deficiency of a phytoplankton community in a coastal jet-front. Mar. Biol. **104:** 329–338.

LEWIS, M. R., J. J. CULLEN, AND T. PLATT. 1984. Relationships between vertical mixing and photoadaptation of phytoplankton: Similarity criteria. Mar. Ecol. Prog. Ser. **15:** 141–149.

LUND, J. W. G., C. KIPLING, AND E. D. LE CREN. 1958. The inverted microscope method of estimating algal numbers and the statistical basis of estimations by counting. Hydrobiologia **11:** 143–170.

MARGALEF, R. 1978. Life-forms of phytoplankton as survival alternatives in an unstable environment. Oceanol. Acta **1:** 493–509.

———, M. ESTRADA, AND D. BLASCO. 1979. Functional morphology of organisms involved in red tides, as adapted to decaying

turbulence, p. 89–94. *In* D. L. Taylor and H. H. Seliger [eds.], Toxic dinoflagellate blooms. Elsevier North Holland.

MOSTAJIR, B., AND OTHERS. 1999*a.* Ecological implications of changes in cell size and photosynthetic capacity of marine Prymnesiophyceae induced by ultraviolet-B radiation. Mar. Ecol. Prog. Ser. **187:** 89–100.

———, AND OTHERS. 1999*b.* Experimental test of the effect of ultraviolet-B radiation in a planktonic community. Limnol. Oceanogr. **44:** 586–596.

MOUSSEAU, L., AND OTHERS. 2000. Effects of ultraviolet-B radiation on simultaneous carbon and nitrogen transport rates by estuarine phytoplankton during a week-long mesocosm study. Mar. Ecol. Prog. Ser. **199:** 69–81.

NEALE, P. J., R. F. DAVIS, AND J. J. CULLEN. 1998. Interactive effects of ozone depletion and vertical mixing on photosynthesis of Antarctic phytoplankton. Nature **392:** 585–589.

NELSON, D. M., J. J. GOERING, AND D. W. BOISSEAU. 1981. Consumption and regeneration of silicic acid in three coastal upwelling systems, p. 242–256. *In* F. A. Richards [ed.], Coastal upwelling systems. American Geophysical Union.

PAASCHE, E. 1980. Silicon content of five marine plankton diatom species measured with a rapid filter method. Limnol. Oceanogr. **25:** 474–480.

PARSONS, T. R., Y. MAITA, AND C. M. LALLI. 1984. A manual of chemical and biological methods for seawater analysis. Pergamon Press.

PRICE, N. M., AND P. J. HARISSON. 1987. Comparison of methods for the analysis of dissolved urea in seawater. Mar. Biol. **94:** 307–317.

REDFIELD, A. C., B. H. KETCHUM, AND F. A. RICHARDS. 1963. The influence of organisms on the composition of sea-water, p. 26–77. *In* M. N. Hill [ed.], The sea. V. 2. Interscience.

SCHEINER, S. M., AND J. GUREVITCH. 1993. Design and analysis of ecological experiments. Chapman and Hall.

SMITH, R. C., AND OTHERS. 1992. Ozone depletion: Ultraviolet radiation and phytoplankton biology in Antarctic waters. Science **255:** 952–957.

SOLÓRZANO, L. 1969. Determination of ammonia in natural waters by the phenolhypochlorite method. Limnol. Oceanogr. **14:** 799–801.

SOMMER, U. 1986. Nitrate- and silicate-competition among Antarctic phytoplankton. Mar. Biol. **91:** 345–351.

TAMIGNEAUX, E., E. VAZQUEZ, M. MINGELBIER, B. KLEIN, AND L. LEGENDRE. 1995. Environmental control of phytoplankton assemblages in nearshore marine waters, with special emphasis on phototrophic ultraplankton. J. Plankton Res. **17:** 1421–1447.

TIAN, R. C., AND OTHERS. 2000. Effects of pelagic food-web interactions and nutrient remineralization on the biogeochemical cycling of carbon: A modelling approach. Deep-Sea Res. II **47:** 637–662.

TREMBLAY, J.-É., L. LEGENDRE, B. KLEIN, AND J.-C. THERRIAULT. 2000. Size-differential uptake of nitrogen and carbon in a marginal sea (Gulf of St. Lawrence, Canada): Significance of diel periodicity and urea uptake. Deep-Sea Res. II **47:** 489–518.

VINCENT, W. F., AND S. ROY. 1993. Solar ultraviolet-B radiation and aquatic primary production: Damage, protection and recovery. Environ. Rev. **1:** 1–12.

VON ENDE, C. N. 1993. Repeated-measures analysis: Growth an other time-dependent measures, p. 113–137. *In* S. M. Scheiner and J. Gurevitch [eds.], Design and analysis of ecological experiments. Chapman and Hall.

WÄNGBERG, S.-Å., K. GARDE, K. GUSTAVSON, AND J.-S. SELMER. 1999. Effects of UVB radiation on marine phytoplankton communities. J. Plankton Res. **21:** 147–166.

WARD, B. B., K. A. KILPATRICK, E. H. RENGER, AND R. W. EPPLEY. 1989. Biological nitrogen cycling in the nitracline. Limnol. Oceanogr. **34:** 493–513.

WHITEHEAD, R., S. DE MORA, S. DEMERS, M. GOSSELIN, P. MONFORT, AND B. MOSTAJIR. 2000. Interactions of ultraviolet-B radiation, mixing, and biological activity on photobleaching of natural chromophoric dissolved matter: A mesocosm study. Limnol. Oceanogr. **45:** 278–291.

ZENTARA, S.-J., AND D. KAMYKOWSKI. 1981. Geographic variations in the relationship between silicic acid and nitrate in the South Pacific Ocean. Deep-Sea Res. **28:** 455–465.

Received: 24 December 2001
Accepted: 13 September 2002
Amended: 24 September 2002